Geotechnical characterization of the soil profile before and after preloading, a case study of soft soils in Durán, Ecuador.

Juan Arévalo-Ochoa
Escuela Superior Politécnica del Litoral, Facultad de Ingeniería en Ciencias de la Tierra, Guayaquil, Ecuador.
jpareval@espol.edu.ec
ORCID: 0000-0001-8006-6621

Steven Muñoz-Buestán
Escuela Superior Politécnica del Litoral, Facultad de Ingeniería en Ciencias de la Tierra, Guayaquil, Ecuador.
hsmunoz@espol.edu.ec
ORCID: 0009-0003-1927-4116

Davide Besenzon
Escuela Superior Politécnica del Litoral, Facultad de Ingeniería en Ciencias de la Tierra, Guayaquil, Ecuador.
besenzon@espol.edu.ec
ORCID: 0000-0002-3384-3747

Carlos Grau-Sacoto
Geocimientos S.A., Guayaquil, Ecuador.
carlosgrau@geocimientos.com

Sara Amoroso
Department of Engineering and Geology, University of Chieti-Pescara, Viale Pindaro 42, 65129 Pescara, Italy; Roma 1 Section, Istituto Nazionale di Geofisica e Vulcanologia, Viale Crispi, 43, 67100 L'Aquila, Italy
sara.amoroso@unich.it
ORCID: 0000-0001-5835-079X

Abstract: The accelerated growth of the industrial zone of Durán, on the Ecuadorian coast close to Guayaquil, requires the construction of structures founded on settlement-powerful strata of soft soils. The high compressibility and low shear strength of these soils create challenges in the stability of the foundations of these structures. The presence of these soils represents a complex geotechnical situation to solve, mainly due to the settlements caused by the magnitude of the overloads from different engineering projects. For the engineering design of the foundation system of any structure, the geotechnical characterization of the subsoil is required to provide reliable resistance and deformability parameters. This article presents the results and interpretation of the in-situ test campaign, complemented with laboratory data, at the Durán Logistics Terminal characterized by these soft deposits. Boreholes with standard penetration tests (SPT), piezocone (CPTU) and seismic dilatometer (SDMT) tests were carried out in different areas, both before and after the application of different preloads useful to induce a part of the settlement before the construction of warehouses. Soil samples allowed to supply soil classification and stiffness characterization, enabling accurate interpretation and correlation with in situ data. The results obtained after the removal of the preloads detect a considerable improvement of the geotechnical parameters due to the induced settlements, providing a helpful case study for the optimal the design of foundation systems in soft deposits.

Keywords: preload; soft soils; geotechnical characterization; in situ tests; piezocone test; seismic dilatometer test.

1. Introduction

In the recent years the Greater Guayaquil region (Ecuador), which includes the city of Durán, has experienced a significant increase of population and industries. This expansion has stimulated the factories to look for alternative areas for their growth, maintaining the crucial connectivity to the Port of Guayaquil. Durán, in response, has evolved rapidly becoming a hub for large industrial complexes, extensive transport networks, storage facilities, and others engineering projects.

Literature concerning nearby areas, including Durán and Guayaquil, indicates that the subsidence of the Quaternary and the corresponding sedimentary fill is related to the contribution of the Guayas River. A very high subsidence rate, coupled with significant soil sedimentation, has resulted in an accumulation of at least 3500 meters of Quaternary deposits (Michaud et al., 2009).

A critical challenge in this region is the prevalence of soft soils, which become particularly problematic for the design of heavy storage facilities that can suffer from differential settlement. These soils tend to dissipate pore pressure over long time, resulting in volume changes and settlements that can adversely affect overlying structures (Fujiwara & Ue, 1990). In this respect, the application of preloads for the improvement of soft soils is a technique extensively used in regions where this issue is recurrent due to its low environmental impact, fast-construction process, and minimal maintenance requirements (Chaiyaput et al., 2023; Kværner & Snilsberg, 2008; Long et al., 2023). The placement of load on the ground surface prior to the construction, facilitates the dissipation of pore pressure, increasing the rates of the primary and secondary consolidation (Mangraviti et al., 2023; Zhang et al., 2023).

This paper focuses on a construction area of new warehouses in Durán Logistics Terminal, characterized by a stratigraphic profile with a considerable thickness of soft soils, potentially including organic soils, peat, and sensitive clays in the estuarine deltaic zone (Paredes & Illingworth, 2022). Due to the soil properties, the use of preloads has been widely employed in this area. In this context, in-situ exploration techniques have been adopted to determine the comprehensive soil characterization of these soft soils deposits, before the application and after the removal of preloads (BAP), particularly using boreholes with standard penetration test (SPT), cone penetration test (CPTu), and seismic dilatometer test (SDMT). Moreover, soil samples were collected for laboratory tests to complement the geotechnical properties of the subsoil and the design of foundation systems.

2. Geological settings

Ecuador is situated in the northwest of South America and represents an active continental margin where the Nazca Plate subducts beneath the South American Plate (Trenkamp et al., 2002). The country is tectonically divided into zones that align parallelly with the arrangement of the northern Andes Mountain Range (Spikings et al., 2000).

In the study area, the soils predominantly represent the Holocene epoch, characterized by an extensive alluvial plain and estuarine deltaic deposits which are positioned at the base of the Chongón-Colonche Mountain Range. Owing to the geological attributes of Guayaquil and Durán, a substantial proportion of its sites exhibit soils prone to liquefaction or a substantial upper layer comprising soft clay and organic material. (Paredes et al., 2022).

The canton of Duran encompasses an approximate area of 59 km^2, located approximately 5 km away from Guayaquil. The topography is predominantly flat, with sporadic isolated elevations, such as the “Las Cabras” hill. The study area corresponds to the industrial zone of Duran, situated just a few meters from the Guayas River. This area, which was previously used for rice cultivation, has not been subjected to significant loads. The study area is depicted in Figure 1.

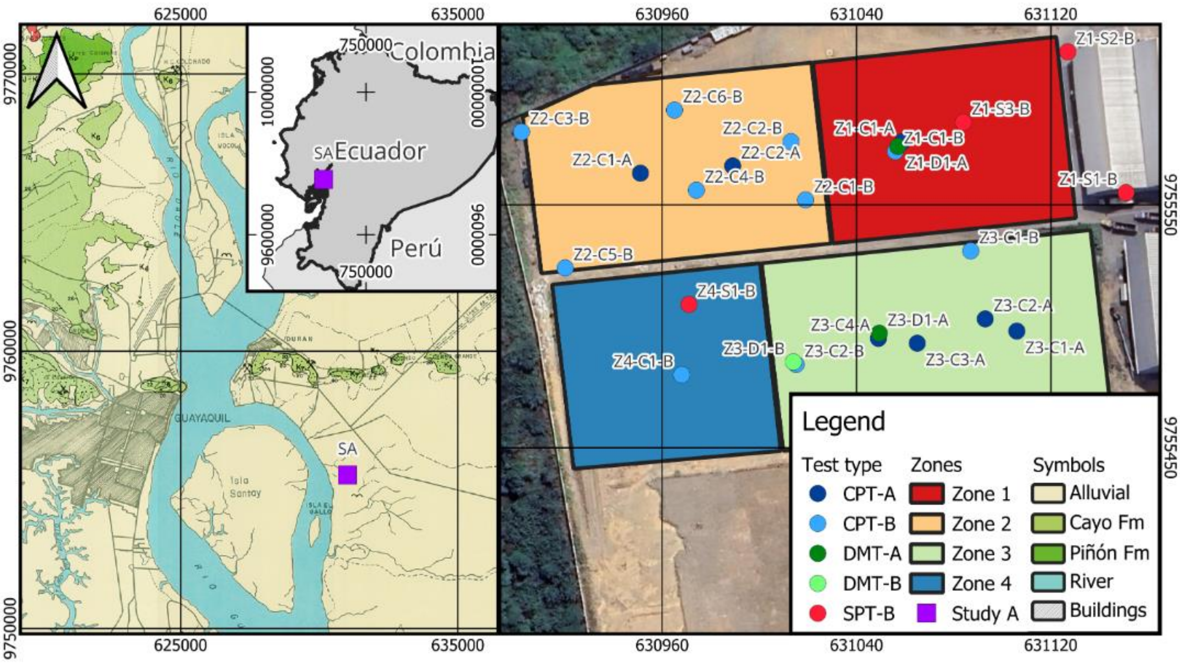

Figure 1. Study Area (SA). The nomenclature assigned to each test corresponds first to the zone number (Z1 to Z4), followed by the initial of the test type (-S for SPT, -C for CPTu, and -D for SDMT) accompanied by the test number (1, 2, 3, etc.), and the initial of the preload stage in which it was conducted (-B for tests before preload and -A for tests conducted after). Geological Map modified from British Mission and Directorate General of Geology and Mines (1979).

The canton of Duran encompasses an approximate area of 59 km^2, located approximately 5 km away from Guayaquil. The topography is predominantly flat, with sporadic isolated elevations, such as the “Las Cabras” hill. The study area corresponds to the industrial zone of Duran, situated just a few meters from the Guayas River. This area, which was previously used for rice cultivation, has not been subjected to significant loads; however, for being near the Guayas River, the upper layers of soils have suffered an increase in the preconsolidation stress, due to the variation of the level of the river.

3. Investigation campaign

During the years 2019 and 2020, there was a preliminary geotechnical exploration campaign of the subsurface in the study area. Three SPTs and one CPTu were conducted in Z1, with Z1-S3-B and Z1-C1-B carried out by an anonymous company, and Geocimientos S.A. conducting the remaining tests and all subsequent ones.

Following the preliminary exploration stage, an additional CPTu and a SDMT after preload (AP) were conducted in Z1. In Z2, six CPTs were performed before preload (BP), and two CPTs were conducted AP. In Z3 BP, two CPTus and one SDMT were executed, while AP involved four CPTus and one DMT. As of the publication of this article, in Z4, one CPTu and one SDMT BP have been carried out.

In total, four SPT tests with a manually hammer drop system, were carried out, resulting in 75 samples for conducting 60 grain-size analyses and 75 Atterberg limits tests. Additionally, undisturbed samples were collected using the Shelby tube, leading to 12 oedometer tests. 18 CPTu tests were performed with a 10cm piezocone at an average depth of 25 m, with data recorded at 0.01 cm intervals. This was complemented by a series of 51 dissipation tests. Three SDMT tests were executed at an average depth of 20 meters, recording data at intervals of 20 cm, and seismic measurements were taken at every 50 cm interval, culminating in five dissipation tests (see Table 1).

Table 1. Summary table of in-situ tests.

Name	Type	Date	East (m)	North (m)	Height (masl)	Phreatic level (masl)	Depth (m)
Z1-S1-B	SPT	17/1/2019	631151	9755555	4.49	2.19	12
Z1-S2-B	SPT	18/1/2019	631127	9755613	4.47	2.17	12
Z1-S3-B	SPT	1/6/2020	631084	9755584	2.59	1.19	40
Z1-C1-B	CPTu	8/12/2020	631056	9755572	4.2	1.6	19.04
Z1-C1-A	CPTu	18/6/2022	631059	9755576	4.21	2.86	25.14
Z1-D1-A	SDMT	1/8/2022	631057	9755574	3.06	1.56	21.2
Z2-C1-B	CPTu	31/8/2021	631019	9755552	3.13	2.63	20.69
Z2-C2-B	CPTu	25/2/2022	631013	9755576	3.39	2.19	20.79
Z2-C3-B	CPTu	3/3/2022	630902	9755580	3.17	2.02	16.75
Z2-C4-B	CPTu	3/3/2022	630974	9755556	3.34	2.59	23.63
Z2-C5-B	CPTu	4/3/2022	630920	9755524	3.25	1.95	22.88
Z2-C6-B	CPTu	12/3/2022	630965	9755589	3.35	2.1	27.62
Z2-C1-A	CPTu	5/4/2023	630951	9755563	2.89	2.89	23.08
Z2-C2-A	CPTu	6/4/2023	630989	9755566	2.77	2.77	23.65
Z3-C1-B	CPTu	2/9/2021	631087	9755530	4.52	2.77	24.6
Z3-C2-B	CPTu	30/7/2022	631013	9755485	2.48	0.78	22.76
Z3-D1-B	SDMT	30/7/2022	631014	9755485	2.5	0.9	20.8
Z3-C4-A	CPTu	11/10/2023	631106	9755498	3.31	1.31	28.25
Z3-C2-A	CPTu	12/10/2023	631093	9755503	3.17	1.17	23.58
Z3-C3-A	CPTu	12/10/2023	631065	9755493	3.14	1.14	21.91
Z3-D1-A	SDMT	12/10/2023	631049	9755497	2.97	0.97	20.3
Z3-C1-A	CPTu	13/10/2023	631049	9755495	2.97	0.97	22.57
Z4-C1-B	CPTu	22/10/2022	630968	9755480	2.5	1.5	19.92
Z4-S1-B	SPT	22/10/2022	630971	9755509	2.64	1.64	15

In total, four SPT tests with a manually hammer drop system, were carried out, resulting in 75 samples for conducting 60 grain-size analyses and 75 Atterberg limits tests. Additionally, undisturbed samples were collected using the Shelby tube, leading to 12 oedometer tests. 18 CPTu tests were performed with a 10 cm piezocone at an average depth of 25 m, with data recorded at 0.01 cm intervals. This was complemented by a series of 51 dissipation tests. Three SDMT tests were executed at an average depth of 20 meters, recording data at intervals of 20 cm, and seismic measurements were taken at every 50 cm interval, culminating in five dissipation tests.

4. Loading bank construction

To address the expansion requirements of the Duran Logistics Terminal and enhance its operational capacity, the management decided for the construction of additional warehouses, designed to support a storage load of up to 5 t/m^2. To limit settlement of the new structure, the consolidation of soil under static pre-load through the construction of an embankment was applied on all the area.

The overall project was divided into five distinct phases, with the initial ground level set at an elevation of +2.60 meters above sea level (masl). As part of the monitoring and control strategy, a system comprising settlement plates was installed. Unfortunately, technical complications hindered the acquisition of continuous and reliable data from these plates. The quantification of total settlement was subsequently achieved through topographic surveys executed post-construction of each loading bank and following its removal.

In the first stage (Z1), a surcharge was placed that reached an elevation of +7.50 masl, applying an approximate load of 91 kPa. The construction took 114 days, with the surcharge application lasting for 331 days. For the second stage (Z2), a taller surcharge was placed, reaching an elevation of +9.30 masl, applying an approximate load of 125 kPa. The construction took 133 days and with a surcharge application lasted for 194 days. In the third stage (Z3) a surcharge was placed that reached an elevation of +9.60 masl, applying an approximate load of 130 kPa. The construction took 102 days, and the surcharge application lasted for 255 days. For the fourth stage (Z4), a surcharge of equal height and load magnitude as in Zone 3 was placed. The construction of this surcharge took 134 days and with a surcharge application lasted for 133 days.

A new stage (Z5) is currently in the process of surcharge construction, with settlements being continuously measured using plates and an electronic measuring instrument. For each zone, the following figures have been created, indicating the stages of loading bank construction and the SPT, CPTu and SDMT tests conducted over time (see Figure 2).

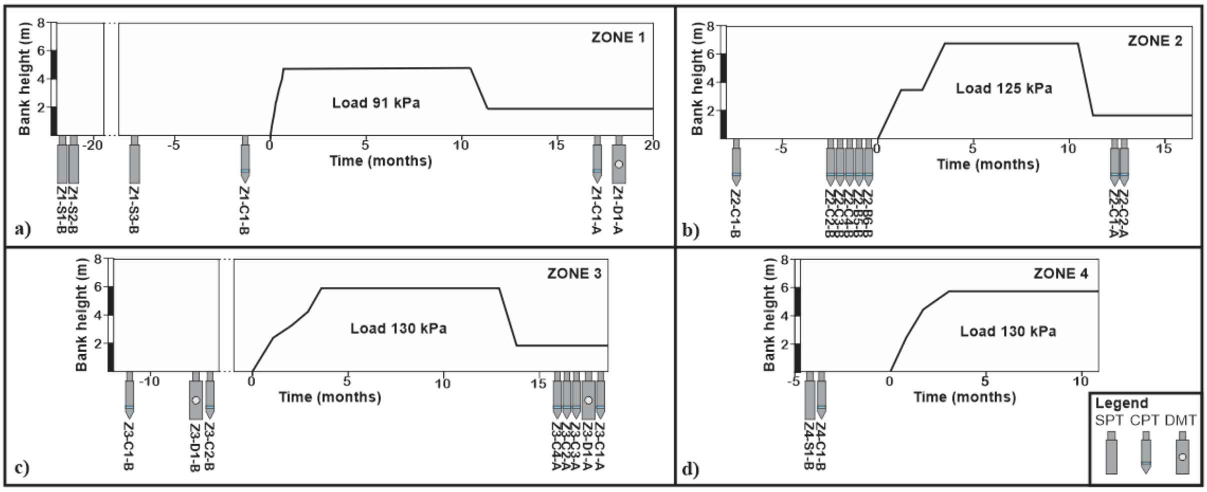

Figure 2. Loading bank construction stages. a) Zone 1, b) Zone 2, c) Zone 3, and d) Zone 4.

5. Geotechnical characterization and soil profile

5.1. SPT, CPTu and SDMT parameters comparisons

SPT, CPTu and SDMT tests were used to measure specific soil parameters BP. These parameters include the corrected cone resistance (q_t), sleeve friction (f_s), and pore water pressure (u_2) for the CPTu test, along with the two corrected pressure readings (p_0, p_1) and the shear wave velocity (V_s) for the SDMT. The results from two representative SDMT and CPTu test are illustrated in Figure 3. The low q_t measurements and the high f_s and u_2 values in the upper 20m of depth, along with the proximity of p_0 and p_1 pressures depth by depth, suggest that most of the soil profile is composed of soft material. Nevertheless, the profile reveals some variability, marked by the presence of sand layers at various depths. The groundwater table (GWT) was estimated to be at a depth of 2.60 meters, as inferred from the u_2 reading of the CPTu test and the third corrected pressure reading (p_2) from the SDMT, when it was available.

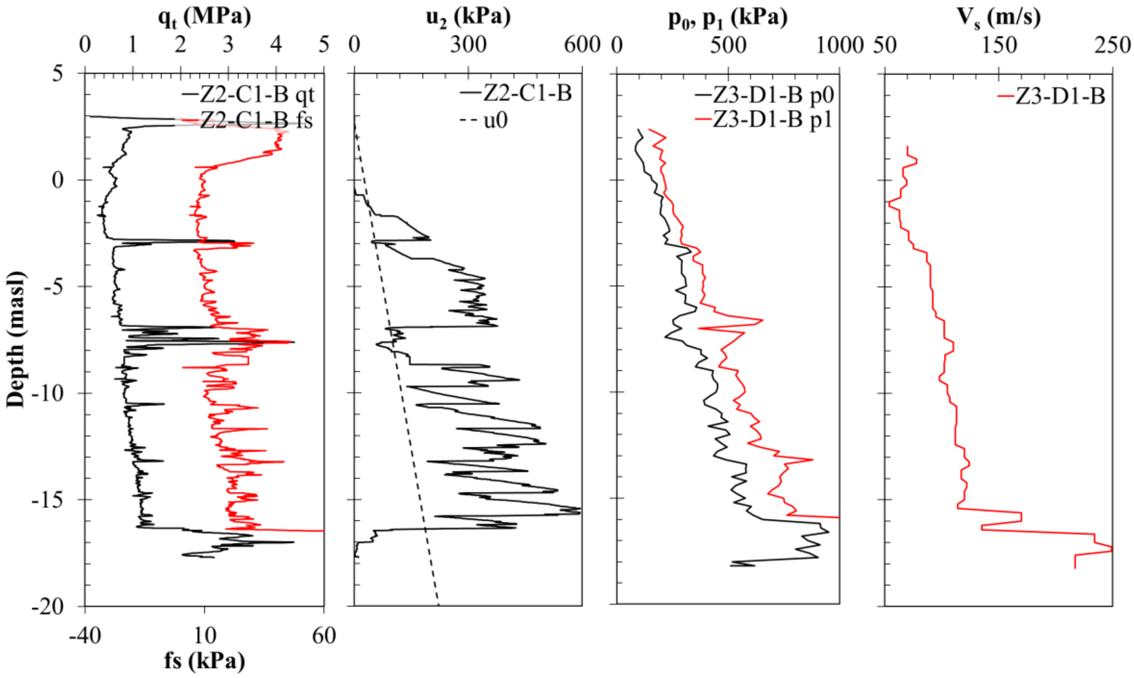

Figure 3. Measured CPTu and SDMT parameters.

CPTu and SDMT tests are often used to estimate compressibility and strength soil parameters. In this respect Robertson (2012) and Marchetti (1980) correlations were employed to determine S_u from CPTu and SDMT tests. It has been noted that the predictions from both tests are quite similar, though there is a slight difference in the initial few meters of depth. This variance might be attributed to a minor difference in the material index I_c and I_D between the two tests.

To assess the overconsolidation ratio (OCR), the notable relationship between K_D and the stress history in clay has underscored the effectiveness of SDMT in providing a stronger estimation of this parameter, using the formula proposed by Marchetti (1980). For fine-grained soils, OCR predictions have also been made using CPTu, based on the normalized q_t values, as indicated by Robertson (2009), and from SPT was estimated from oedometer tests. It can be observed that there is a consistent shift across all depths between the CPTu and SDMT predictions, with oedometer calculus being the minor with consistent values from SDMT, and with the CPTu prediction generally being higher than that of the SDMT.

Results from penetration tests are widely utilized for estimating soil settlement by applying the constrained modulus (M). This modulus is influenced by factors like the stress state, soil type, and the OCR. Several research endeavors have sought to assess the constrained modulus through diverse in-situ penetration tests, recognizing it as a straightforward and efficient property for evaluating deformation characteristics (Lee et al., 2010; Lunne & Christoffersen, 1983). Constrained modulus from SPT was based on the results of the oedometer consolidation test, for the CPTu, it was estimated using Robertson (2009), and for SDMT was estimated using Marchetti et al. (1980). Comparisons are shown in Figure 4.

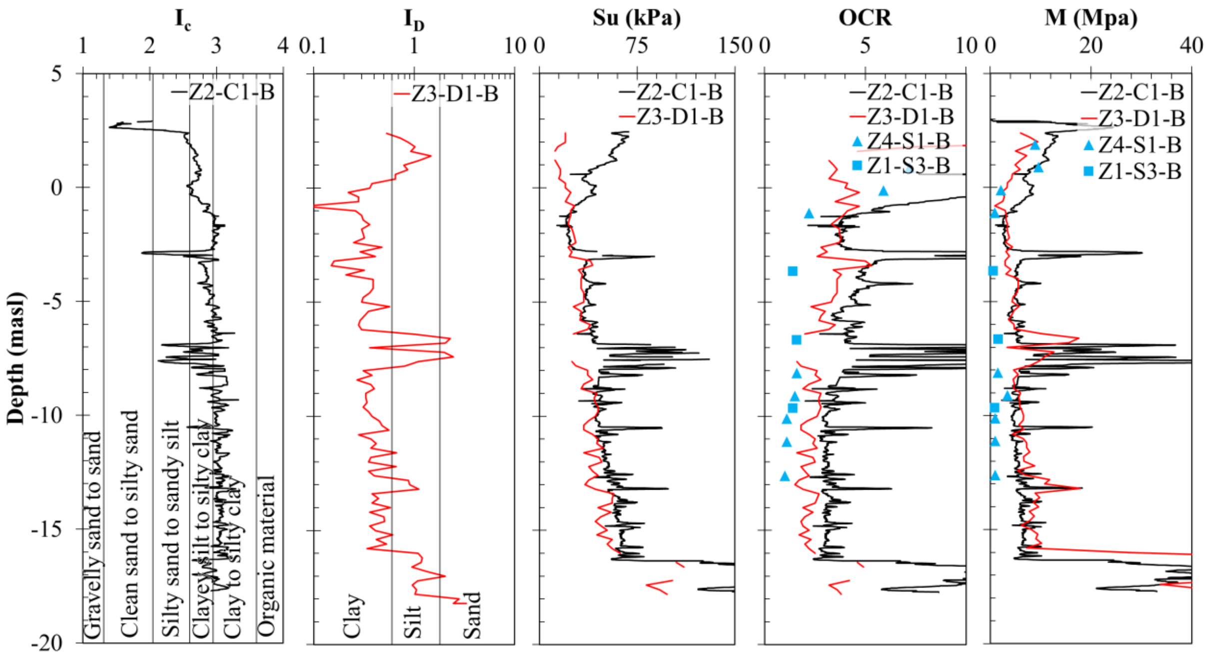

Figure 4. Estimated CPTu and SDMT parameters.

In Figure 5 were plotted % composition of materials from test Z1-S3-B (which is the deeper test executed), as well as the liquid limit LL, plastic limit PL, plasticity index PI, and moisture content w. For test Z1-C1-B, the segmented I_c values were located, with values: >3.6 for organic soils, 2.50 to 3.60 for clays and silty clays, 2.60 to 2.95 for silty clay loam and silty clays, 2.05 to 2.60 for silty sand and sandy silt, 1.31 to 2.05 for clean sand to sandy silt, and <1.31 for gravelly sand and dense sand (Robertson & Cabal, 2022). From test Z4-D1-B, the segmented I_D values were located, with 0.1 to 0.6 for clays, 0.6 to 1.8 for silts, and >1.5 for sands (Marchetti et al., 2001).

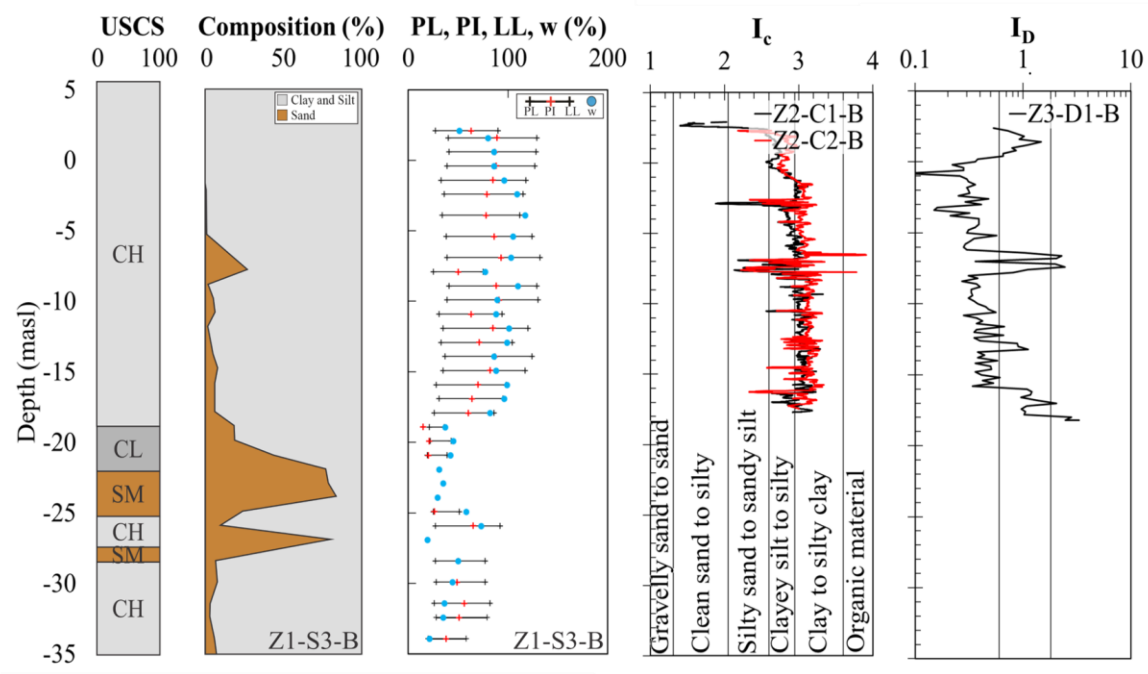

Figure 5. Combined representation of SPT, CPTu, and SDMT for the stratigraphic profile.

A substantial layer of high plasticity clay (CH) was prominently identified, according to the Unified Soil Classification System (USCS) nomenclature provided by the SPT test, extending to at least 24 meters. An interesting double-layer intercalation of approximately 1 meter and 50 cm of sand mixtures was observed at depths of -4.0 and -7.5 meters above sea level (masl), respectively.

Additionally, a silt lens was observed at -15 masl, followed by a layer of low plasticity clay (CL) at approximately -18 masl. A similar trend is depicted in the stratigraphic section in Figure 6 and Figure 7. Similar representations have been reported by other authors (Álvarez et al., 2022; Cavallaro, 2022; Fakharian et al., 2022; Ripalda et al., 2022). From the SPT tests, it was observed that at approximately -22 masl, there is a rigid double layer of quite consistent sandy material. However, below this material, a high plasticity clay layer is encountered again.

Two cross-sections were created too, designated as 1-1’ (Figure 6) and 2-2’ (Figure 7). Here we plotted I_c and q_t values for CPTu tests; Plastic Index (PI) and Standard Penetration Resistance (N_{SPT}) for SPT tests; and I_D and K_D values for SDMT test. The plotted boreholes correspond to tests conducted BP.

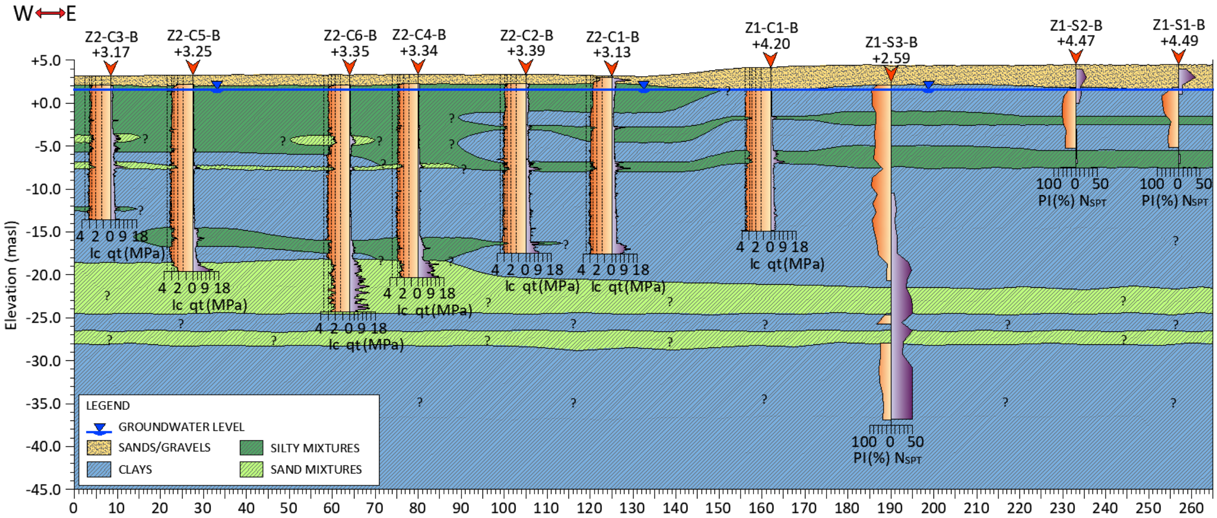

Figure 6. Cross-section 1-1’.

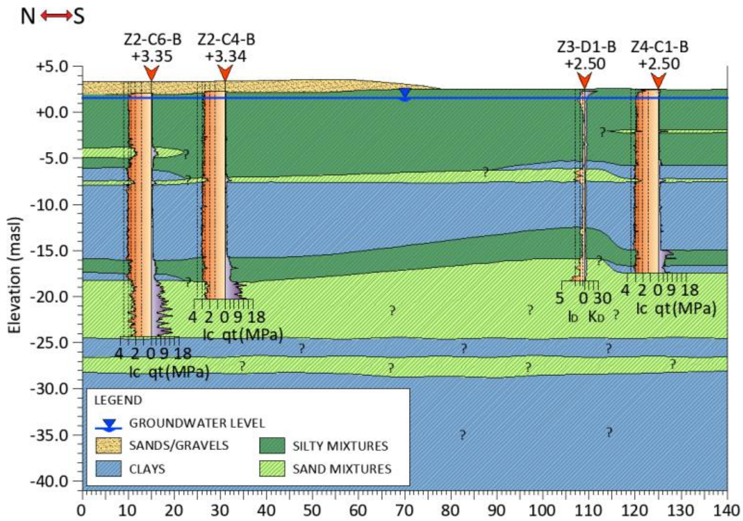

Figure 7. Cross-section 2-2’.

Based on Figure 6 and Figure 7, the study area reveals a surface soil fill consisting of gravels and sands, succeeded by alternating layers of clays and silty mixtures, with a depth ranging from 20 to 24 meters. Moreover, in the western sector, there are sand mixtures lenses between layers of clays and silty mixtures. Subsequently, there is a layer of sand mixtures, with its thickness increasing from 3 meters in the eastern sector to 6 meters in the western sector. From borehole Z1-S3-B, it is assumed that beneath the sand mixtures layer and throughout the entire study area, there is a 2-meter-thick layer of clays, followed by a 1.5-meter-thick layer of sand mixtures, and then a substantial stratum of clays up to 10 meters in thickness.

5.2. Comparison of pore pressure dissipation tests

To estimate the k_h parameter from CPTu we used Equation 1 and c_h was estimated with Equation 2 (Robertson, 2010). Results were plotted in Figure 8.

$$k_h = \begin{cases} 10^{0.952-3.04\,I_c}, & 1.0 < I_c \leq 3.27 \\ 10^{-4.52-1.37\,I_c}, & 3.27 < I_c < 4 \end{cases} \qquad (1)$$

$$c_h = \frac{k_h * M}{\gamma_w} \qquad (2)$$

For CPTu dissipations, the t_{50} values were obtained from the dissipation tests, tracing a tangent line to the initial portion of the dissipation curve and calculation the midpoint between the assumed initial pore pressure u_i and the pore pressure at that depth u_0, as suggested in (Robertson, 2010; Robertson & Cabal, 2022). With t_{50} determined, the horizontal consolidation coefficient c_h were estimated using Equation 3. Results were plotted in Figure 8.

$$c_h = \frac{T * r^2 * I_r^{0.5}}{t_{50}}, \quad with \begin{cases} Theoretical\ time\ factor\ T: 0.245 \\ Penetrometer\ radius\ r = 0.0178m \\ Soil\ Rigidity\ Index\ I_r \end{cases} \qquad (3)$$

For SDMT dissipation test, the contraflexure time t_{flex} occurs on the contraflexure point from the dissipation curve, and parameter c_h can be estimated from Equation 4 (Marchetti et al., 2001). With c_h, horizontal permeability k_h can be determined with Equation 5. These results were plotted in Figure 8.

$$c_h = \frac{7cm^2}{t_{flex}} \qquad (4)$$

$$k_h = \frac{c_h * \gamma_w}{M} \qquad (5)$$

A total of 12 samples for consolidations were obtained from two SPT tests (Z4-S1-B and Z1-S3-B). From this, the vertical consolidation coefficient c_v, vertical permeability k_v, preconsolidation pressure σ'_p, compression index C_c, swelling index C_s, and OCR were determined (Terzaghi, 1925; Terzaghi & Peck, 1967). Results were plotted in Figure 8.

For the comparison of the consolidation coefficient all tests were plotted BP, c_h from a CPTu (Z2-C2-B) with his dissipation (Z2-C2-B diss), the c_h from SDMT dissipation (Z3-D1-B diss) and the calculated c_v from SPT's (Z4-S1-B and Z1-S3-B). In the same way as previous, for the comparison of permeability were plotted, the k_h from CPTu BP (Z2-C2-B) with his dissipation (Z2-C2-B diss), the k_h from SDMT dissipation BP (Z3-D1-B diss), and the estimated k_v from SPT's BP (Z4-S1-B and Z1-S2-B) (see Figure 8).

It should be noted that the tests were compared for Zone 3, where the highest quantity and reliability of tests are available. However, it is important to acknowledge that the SPT tests correspond to different zones, and as such, variations in behavior would be anticipated due to the distinct geological characteristics of these zones.

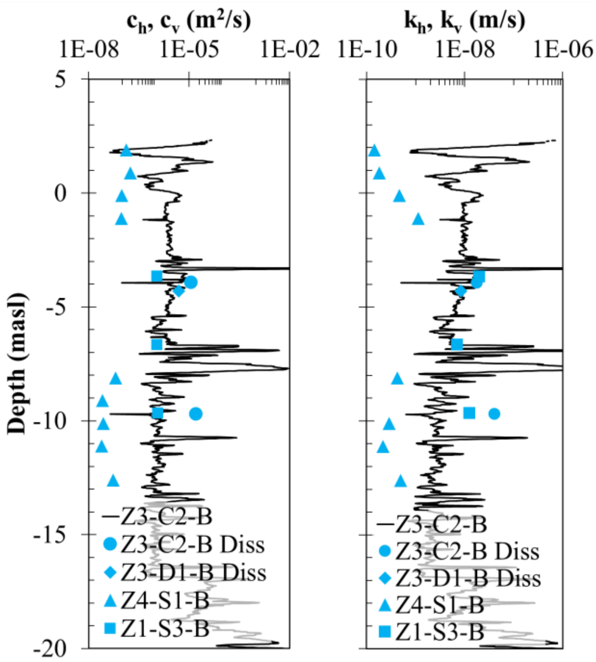

Figure 8. Consolidation coefficients and permeability coefficients estimated from CPTu continuous, CPTu dissipation, SDMT dissipation and SPT oedometer consolidations.

In the case of consolidation coefficients, c values from CPTu continuous are like SDMT dissipation and SPT Z1-S3-B results, CPTu dissipation values are higher, and SPT Z4-S1-B are lower. A similar trend to the one mentioned is observed for the permeability coefficients.

It should be considered that not all tests correspond to Zone 3, and furthermore, the SPT tests conducted in the oedometers calculate vertical consolidation and permeability coefficients, while the other tests estimate horizontal coefficients. This difference in coefficient orientation may influence the comparisons and should be considered when interpreting the results.

5.3. Estimation of fine content from geotechnical in-situ tests

An estimation of the fine content (FC) was conducted between SPT, CPTu, and SDMT tests BP. The fine content of borehole Z1-S4-B was related to the I_c index of borehole Z1-C1-B, using the Boulanger & Idriss (2014) method (Equation 6) and Suzuki et al. (1998) method (Equation 7). For borehole Z1-D1-B was related to the I_D index using Di Buccio et al. (2023) method (Equation 8). The results obtained from each method were plotted in Figure 9.

$$FC = 80\,(I_c + C_{FC}) - 137 \quad (6)$$

$$FC = x_c\,(2.8\,Ic^{2.6}) \quad (7)$$

$$FC = X_D\,(-31\,I_D + 91) \quad (8)$$

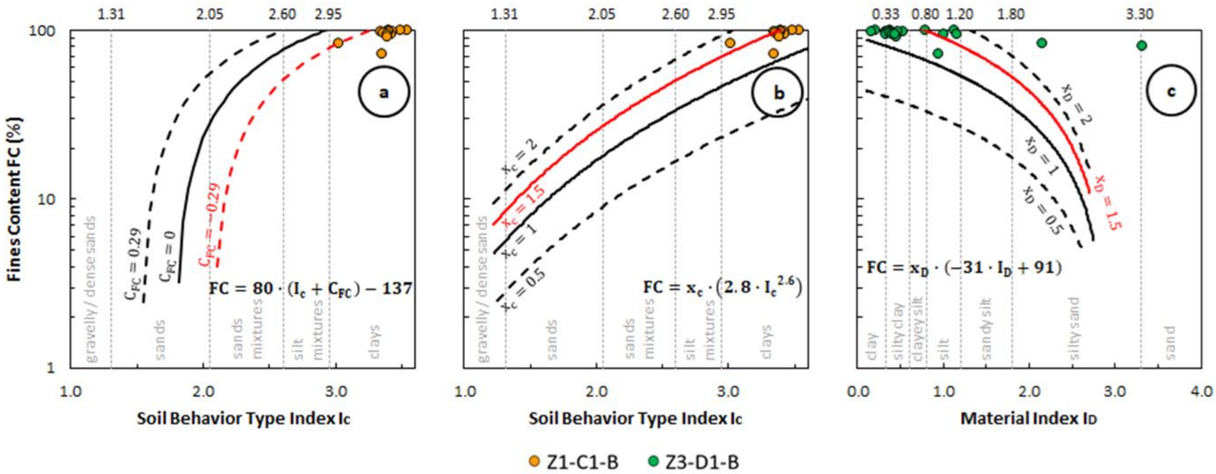

Figure 9. Fine content estimations: (a) I_c-FC chart by Boulanger & Idriss method; (b) I_c-FC chart by Suzuki et al. method; (c) I_D-FC chart by Di Buccio et al. method.

Figure 21a-b shows little variability in the C_{FC} values, mainly in the range of -0.29 to -0.35 and in the range of 1 to 2 for the x_c coefficient. The best fit shows a negative value of C_{FC} = -0.29 for Boulanger & Idriss method, x_c = 1.5 for Suzuki et al. method, and x_D = 1.5 for Di Buccio et al. method. These values may be useful for indirect FC estimates obtained in further investigations in these areas, using the following expressions respectively (Equation 9 to Equation 11).

$$FC = 80\,(I_c - 0.29) - 137 \quad (9)$$

$$FC = 1.5\,(2.8\,I_c^{2.6}) \quad (10)$$

$$FC = 1.5\,(-31\,I_D + 91) \quad (11)$$

For FC estimates from CPTu tests, the coefficient x_c = 1.5 obtained from the Suzuki et al. method provides a fines content (FC) profile that fits better to the laboratory data than the coefficient obtained by the Boulanger & Idriss method (C_{FC} = -0.29). This is confirmed by comparing the overall standard deviation (Equation 12), of the FC predictions with respect to the FC value measured in the laboratory:

$$SD = \frac{\sqrt{(FC_{CPT} - FC_{LAB})^2}}{N} \qquad (12)$$

Where FC_{CPT} is the FC prediction obtained by CPTu correlations, FC_{LAB} is the FC value measured in the laboratory and N the total number of measurements (Di Buccio et al., 2023). In the study area, the overall standard deviation obtained by the Suzuki et al. method is lower than obtained by the Boulanger & Idriss method (2.2% and 4.4% respectively), allowing a better correlation with the laboratory data. While, with the method proposed by Di Buccio et al., the overall standard deviation for the SDMT correlation is 6%, similar to the CPTu correlations.

6. Geotechnical monitoring of tests

6.1. Comparison of CPTu tests conducted BAP

Due to soil compression during the AP phase, the stratigraphy of BP and AP boreholes does not correspond in the initial meters and tends to align at greater depths. Therefore, comparisons were made with different depths, as shown in Table 2.

To facilitate comparisons between CPTu tests conducted BAP, the measured parameters q_t, f_s, and the estimated I_c were examined between nearby tests within the same study zone. In Zone 1, a suitable pair of tests for comparison could not be identified due to discrepancies in the values obtained from CPTu tests, especially in I_c. In Zone 2, a pair of tests, Z2-C6-B and Z2-C1-A, located at a proximity of 30 m with homogeneous parameters, allowed for the first comparison (CZ2-I). Similarly, in Zone 3, two pairs of tests, Z3-C2-B with Z3-C4-A (CZ3-I) and Z3-C1-B with Z3-C2-A (CZ3-II), were found at distances of 28 m and 35 m, respectively. No comparisons could be made for Zone 4 as the preload has not been removed at this point.

The three comparisons (CZ2-I, CZ3-I, and CZ3-II) were graphically represented in Figure 10 to Figure 12, focusing on parameters of interest such as I_c, q_t, S_u, OCR, and M, based on the clay behavior of the analyzed soil profile.

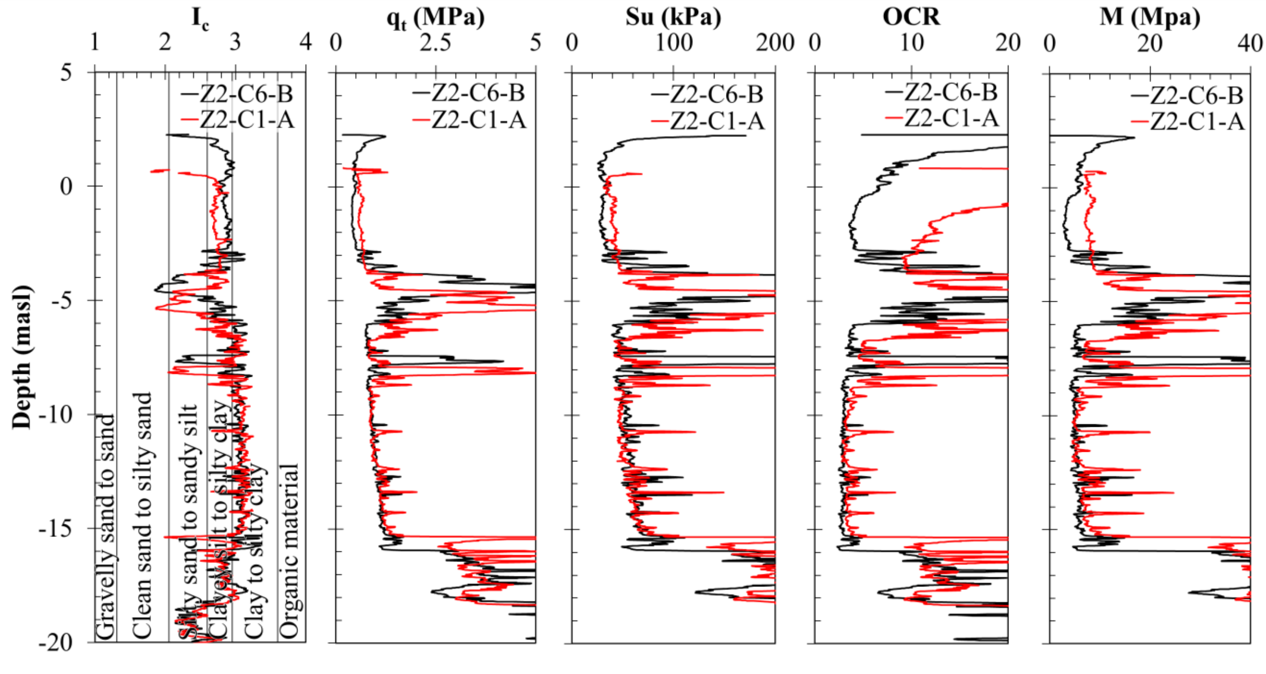

Figure 10. CZ2-I. Comparison of CPTu tests conducted in Zone 2 BAP.

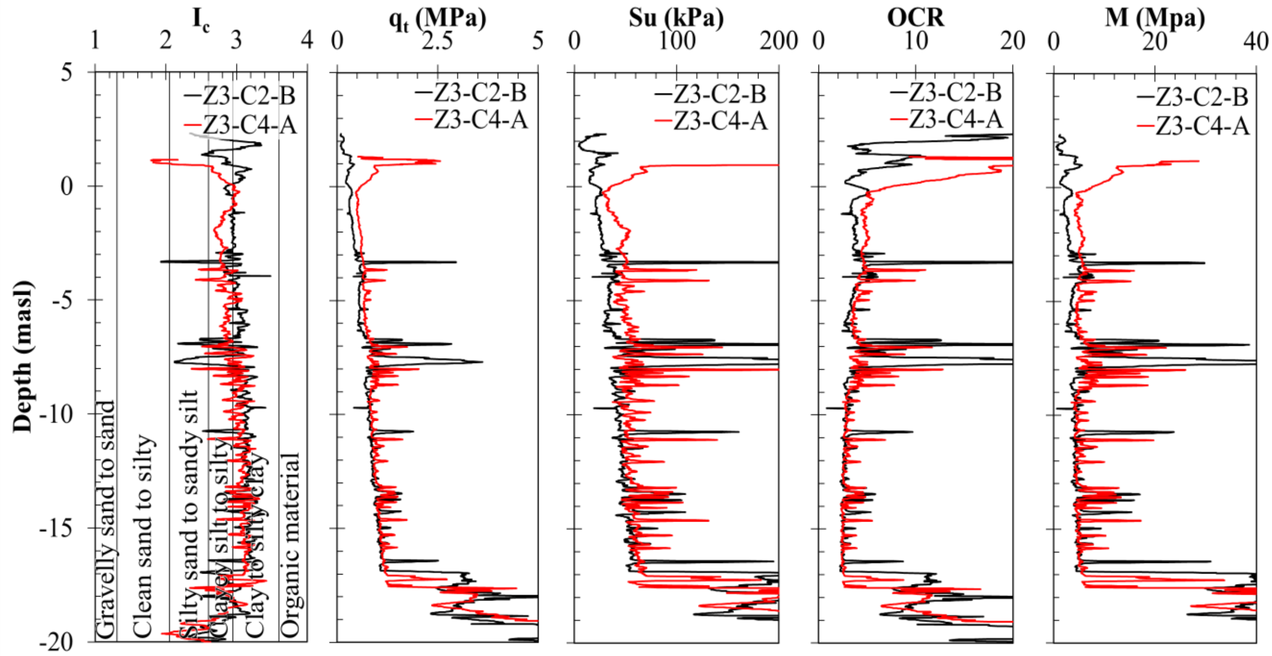

Figure 11. CZ3-I. Comparison of CPTu tests conducted in Zone 3 BAP.

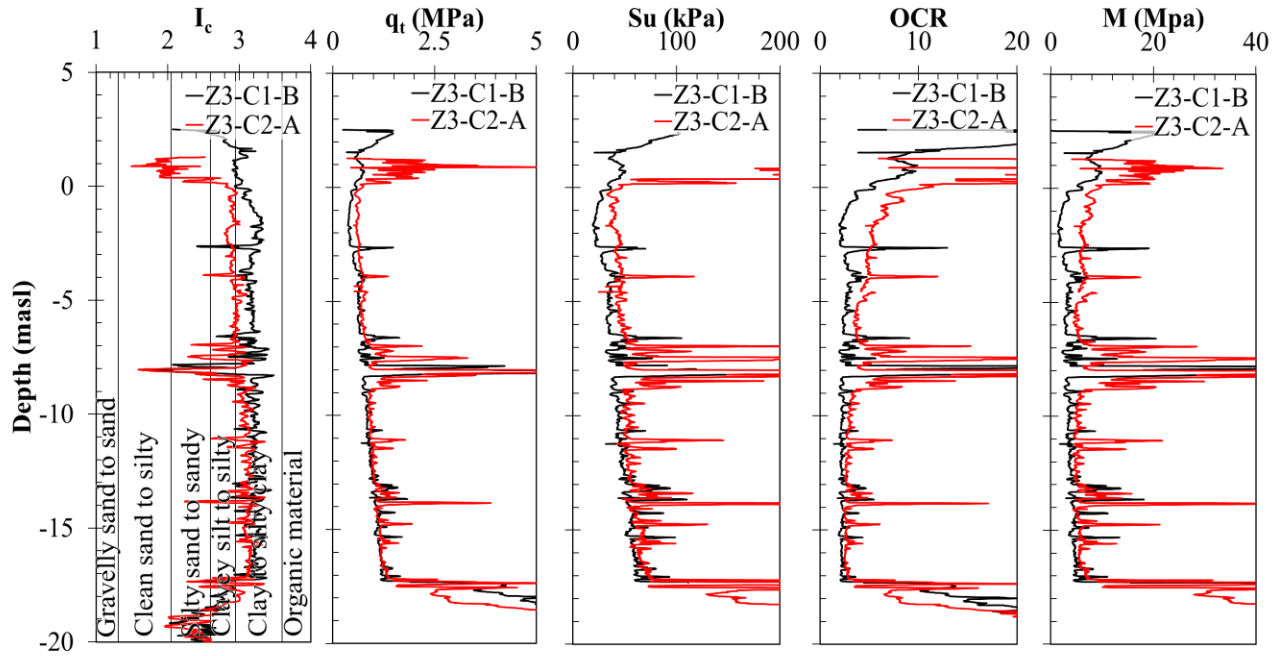

Figure 12. CZ3-II. Comparison of CPTu tests conducted in Zone 3 BAP.

Table 2 displays the percentage variation of the plotted parameters, where the stratigraphy was divided into three significant segments: the first segment of clay beneath the surface, followed by a layer or double layer of sand, and the third segment corresponding to another extensive layer of clay, before reaching the sand layer located at approximately -20 meters above sea level.

To determine the percentage variation of the parameters before and after applying preloads, the mean trimmed of each parameter was calculated using the Equation 13.

$$\bar{\chi} = \frac{\sum_{i=p+1}^{n-p} \chi_{(i)}}{n-2p} \qquad (13)$$

The examination of post-preload tests reveals a discernible 'enhancement' across all parameters, particularly within the initial meters of the subsurface, corresponding to the uppermost clay layer which are described below.

Notably, the I_c parameter, theoretically expected to remain constant, demonstrates variations. In CZ2-I and CZ3-I, the clayey materials exhibit a tendency toward silt, with a variation in this section around -5% and -4% for both zones; in CZ3-II, clay to silty clay materials exhibit a tendency toward clayey silt to silty clay, with a variation of approximately -7%. Concerning the q_t parameter, its variation was anticipated due to mineralogical compression of the soil. In CZ2-

I, CZ3-I, and CZ3-II, a similar behavior is observed with a variation of 42%, 35% and 19%, respectively, within the same initial clay stage.

The S_u parameter displays a comparable trend across the three zones, with variations in the first stage of approximately 34%, 60% and 37%, respectively. CZ2-I exhibits a higher S_u value compared to CZ3-I and CZ3-II, where it is practically similar. OCR, a crucial parameter for comparison, indicates over-consolidation due to preload, necessitating a higher value in AP than BP especially in the first clay layer. CZ2-I shows a variation around 177%, the highest among the three tests. CZ3-I presents the lowest variation of 19% while CZ3-II demonstrates a variation of approximately 58%. The M parameter follows a similar trend across zones, with variations of 53%, 57% and 78% for each respective zone in first described layer. The parameter M/q_t shows a variation of up to 7%.

The second layer shows little variability in the I_c parameter, except for CZ3-II, where there is a variation of up to -27%. In the q_t parameter a variation of up to -29% is observed, while S_u varies from 8% to 21%, with a significant increase in CZ3-II where the variation reaches 53%. For CZ2-I, the OCR shows a notable increase, reaching a variation of up to 68%, while in CZ3-I, the parameter decreases by -33%. The modulus M varies from 23% to 36%. In this layer, the parameter M/q_t decreases by -15%.

For the bottom layer, there are minor variations. The I_c parameter exhibits almost no change, with variations between 2% to -4%. The q_t parameter shows a variation of less than -12%, while the undrained shear strength varies between 10% and 21%. The variation in OCR is less than -2%; however, in CZ3-II, this variation reaches a value of 23%. The modulus M varies from 8% to 20%. In this layer, the parameter M/q_t increase by 19%.

Table 2. CPT variation parameters in percent

Zone	Tests before		Tests after		Parameters											
	Test	DI (masl)	Test	DI (masl)	I_c, I_D		q_t, K_D		S_u		OCR		M		M/q_t	
					MTB	MTA	MTB	MTA	MTB	MTA	MTB	MTA	MTB	MTA	MTB	MTA
2	Z2-C6-B	1.4;-2.7	Z2-C1-A	0.4;-3.6	2.9	2.7 (-5%)	0.4	0.6 (42%)	30.7	41.1 (34%)	5.3	14.7 (177%)	4.4	8 (83%)	-	-
		-2.7;-8.7		-3.6;-9.1	2.8	2.7 (-2%)	1.3	1.6 (24%)	89.7	108.2 (21%)	9.7	16.4 (68%)	14.7	20 (36%)	-	-
		-8.7;-17.7		-9.1;-15.1	3	3.1 (2%)	1.2	1.1 (-12%)	68.8	56.3 (-18%)	3.5	3.5 (0%)	8	6.7 (-17%)	-	-
3	Z3-C2-B	0.5;-6.5	Z3-C4-A	-0.2;-6.7	3	2.8 (-4%)	0.5	0.6 (35%)	29.6	47.3 (60%)	3.7	4.4 (19%)	3.3	5.1 (57%)	-	-
		-6.5;-8.5		-6.7;-8.7	2.9	3 (3%)	1.1	0.9 (-13%)	72.4	58.3 (-19%)	6.6	4.4 (-33%)	11.3	7.7 (-32%)	-	-
		-8.5;-16.5		-8.7;-16.7	3.1	3.1 (-2%)	0.9	1 (7%)	49.7	57.1 (15%)	2.7	2.8 (1%)	4.6	5 (8%)	-	-
	Z3-C1-B	1.5;-6.5	Z3-C2-A	0.2;-6.8	3.1	2.9 (-7%)	0.6	0.7 (19%)	32.4	44.3 (37%)	3.2	5 (58%)	3.5	6.3 (78%)	-	-
		-6.5;-8.5		-6.8;-8.8	3.1	2.8 (-7%)	1	0.7 (-29%)	46.1	49.7 (8%)	4.1	4.7 (17%)	7.8	5.9 (-25%)	-	-
		-8.5;-17		-8.8;-16.8	3.2	3.1 (-4%)	1	1 (-1%)	52	57.1 (10%)	2.2	2.8 (23%)	4.2	5 (19%)	-	-

Z3-D1-B	-0.1;-5.6	Z3-D1-A	0.7;-5.3	0.3	0.4 (22%)	4.5	4.4 (-3%)	28.4	36.5 (29%)	3.5	3.4 (-4%)	3.7	5.9 (60%)	-	-
	-5.6;-7.6		-5.3;-8.3	1.1	0.8 (-27%)	3	3.6 (19%)	29.8	45.6 (53%)	2.2	2.7 (24%)	9.5	11.8 (23%)	-	-
	-7.6;-15.1		-8.3;-15.3	0.4	0.4 (-4%)	3.3	3.3 (0%)	43.6	52.9 (21%)	2.2	2.2 (-2%)	7.2	8.7 (20%)	-	-
Z3-C1-B Z3-D1-B	2.9;-5.1	Z3-C2-A Z3-D1-A	0.7;-5.3	-	-	-	-	-	-	-	-	-	-	7.1	7.6 (7%)
	-5.1;-8.1		-5.3;-7.8	-	-	-	-	-	-	-	-	-	-	9	7.6 (-15%)
	-8.1;-15.1		-7.8;-15.3	-	-	-	-	-	-	-	-	-	-	7.4	8.9 (19%)

DI: depth interval, MTB: mean trimmed before, MTA: mean trimmed after.

6.2. Comparison of SDMT tests conducted BAP

For the comparison of SDMT BAP tests, parameters such as I_D, k_D, S_u, OCR and M were contrasted (Figure 13) because, like CPTu, these parameters provide an accurate characterization of the soil being worked on. However, here we compare V_s, Go and M/qt parameters too (Figure 14). At the time of this publication, SDMT BAP tests were conducted only in Z3 (Z3-D1-B and Z3-D1-A).

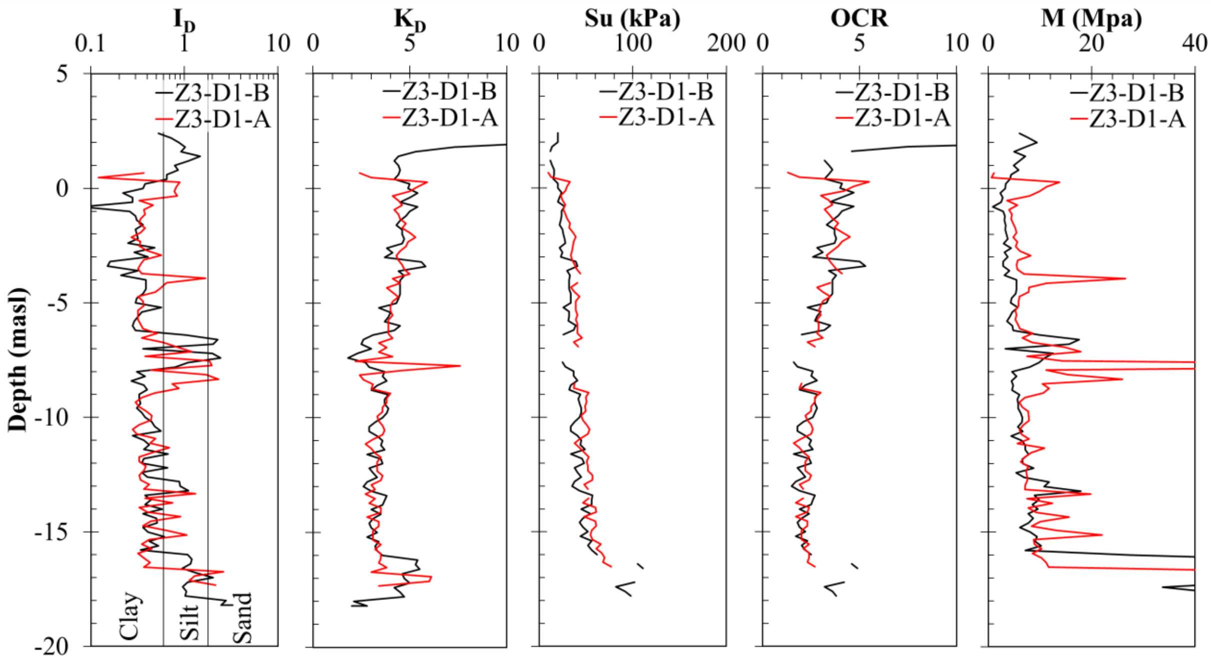

Figure 13. Comparison 1 of SDMT tests conducted in Zone 3 BAP.

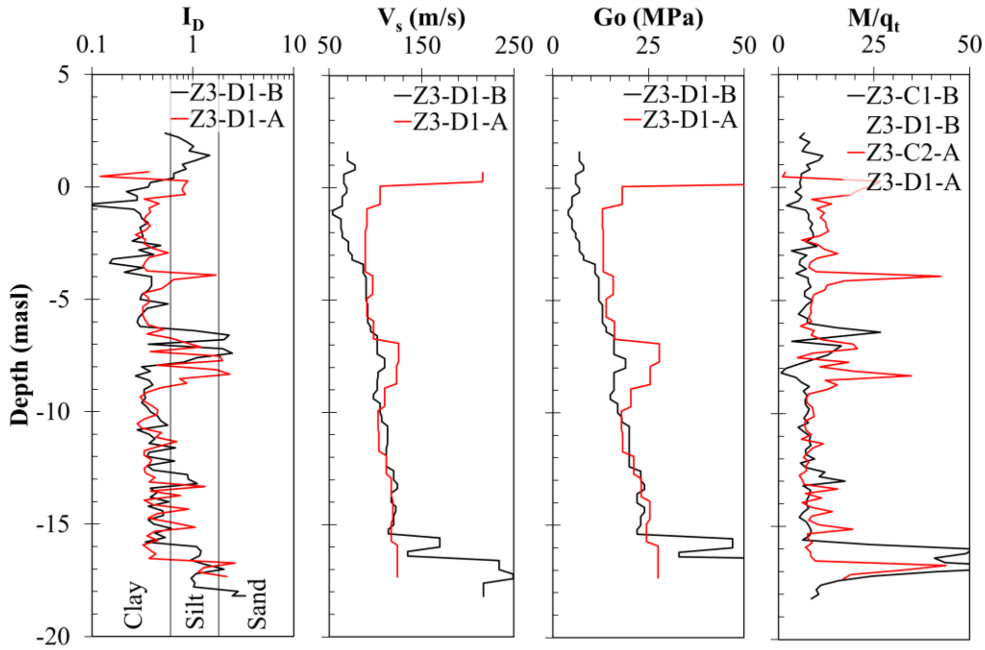

Figure 14. Comparison 2 of SDMT tests conducted in Zone 3 BAP.

As shown in Figure 13 and Table 2, in the first layer, I_D increase by 22% and after the sand layer appears to remain relatively constant. K_D parameter does not exhibit a significant numerical change except in the sand layer. As expected, the S_u parameter shows a slight increase, which is noticeable in the first 6 meters of clayey material, where it exhibits a variation of approximately 29%. The OCR evaluation, unlike the CPTu estimates, does not indicate an increase, which is unexpected as it should be higher for AP tests. Conversely, the M parameter shows an increase of around 60% in the first layer.

7. Behavior of the simplified model in Plaxis

To estimate settlements in this area, a simplified model (Figure 15) was created in Plaxis using an embankment with a height of 7 m and 100 m width, constructed over a soil profile with dimensions of 500 m in width and 100 m in depth, consisting of 3 materials: Clay 1 from 0 to 25m, Sand from 25 to 35m and clay 2 from 35 to 100m and a phreatic level at 1m. The material properties are shown in Table 3.

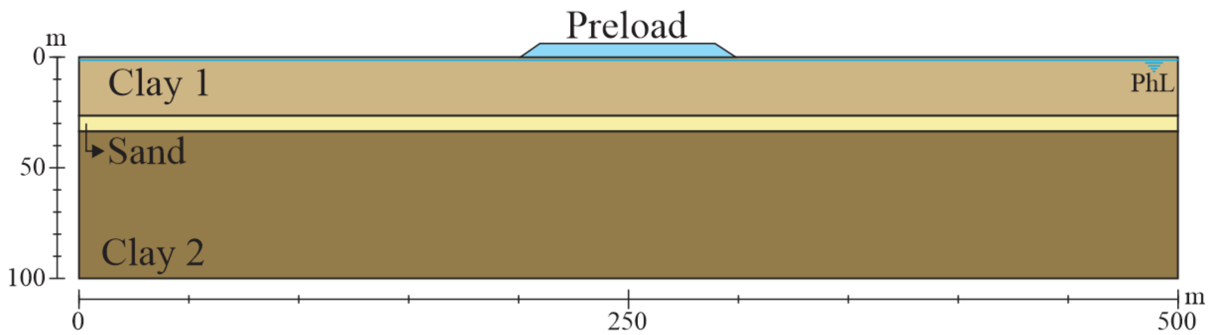

Figure 15. Geometry Plaxis Model

Table 3. Materials properties

Material	Clay 1	Sand	Clay 2
Type	Undrained A	Drained	Undrained A
γ unsat (kN/m^3)	17	19	17
γ sat (kN/m^3)	18	20	18
C (kPa)	50	10	50
ϕ (°)	15	35	15
E (kPa)	4829	30000	20000
k (m/s)	1.00E-08	1.00E-06	1.00E-08

For the analysis we divide the computation in three stages: a) Construction of soil profile with gravity load calculation, b) Consolidation in construction of the preload which was constructed in 50 days and was calculated with consolidation type and c) Consolidation with preload completed which was calculated with consolidation type for 2 sceneries: 1) One year AP construction and 2) At 90% final consolidation. Vertical displacements by stages were plotted for stage 2 (50 days) (Figure 16), stage 3 one-year AP construction (Figure 17) and for 90% of final consolidation (Figure 18).

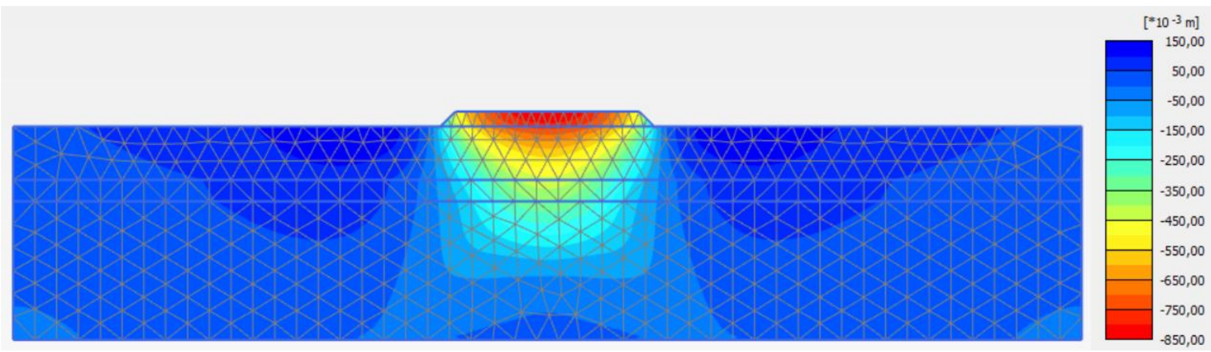

Figure 16. Partial settlements at finish construction preload (50 days)

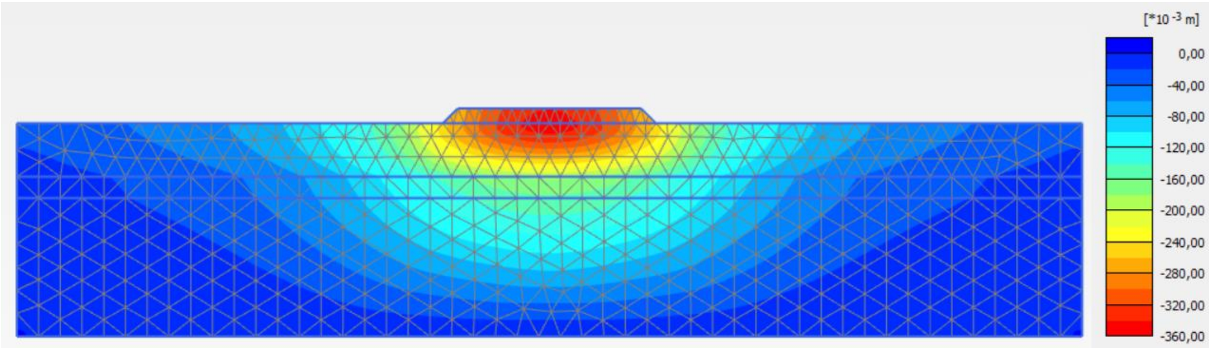

Figure 17. Partial settlements one year AP construction

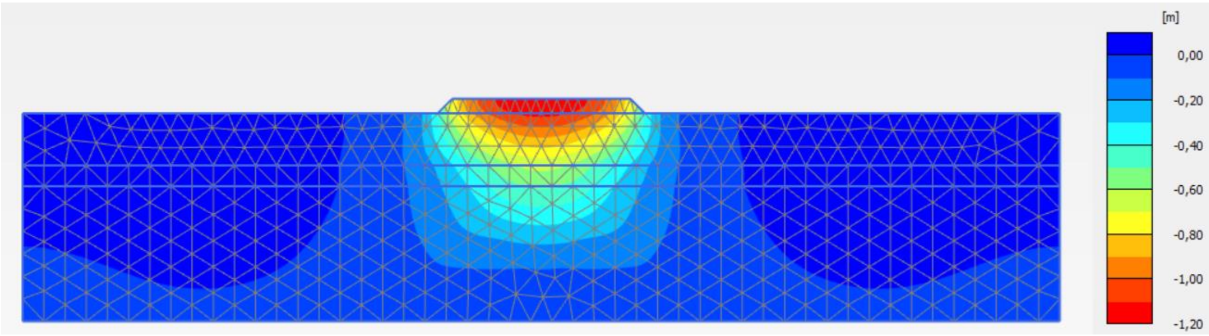

Figure 18. Total vertical displacements at 90% final consolidation (648 days)

From Figure 16, it can be observed that there is a construction settlement of approximately 85cm, which is achieved in the 50 days during the construction of the embankment. In Figure 17, once the preload is constructed, settlements reach 36cm, which are achieved one year after the completion of the construction. Finally, from Figure 18, it is observed that settlements reach 90% consolidation at 648 days, with a maximum settlement of around 120cm, indicating that 1 year and 50 days later, there is no significant variation in settlements compared to the 90% of final consolidation.

Two key points should be highlighted. Firstly, beyond the sand layer that is not penetrated by either CPTu or SDMT tests, there still exists a clay layer representing a significant volume within which settlements continue to occur. These settlements might be going unnoticed and not considered. Secondly, it is crucial to note that most settlements occur during the construction of the preload. Therefore, monitoring settlements during construction is indispensable for effective settlement control.

8. Conclusions

Given the quantity and quality of tests conducted in this study, the results exhibit a high degree of replicability, leading to the following conclusions:

Since the construction of an embankment creates significant stresses in the first few meters of the soil upon which it is placed, the physical parameters of that section tend to exhibit the greatest variation. Consequently, at greater depths, the parameters tend to behave similarly.

Preloading has demonstrated the capacity to enhance fundamental soil parameters such as S_u, and M, showing an average (both CPTu and SDMT) increase of 40% and 70%, respectively. This enhancement is evident in the comparative analysis of CPTu and SDMT tests.

Although I_c, a parameter not expected to change after preload, exhibits a variation, the I_D parameter also shows a minimal increase.

The OCR parameter experiences substantial increases, aligning with expectations in CPTu estimations (85%). However, in SDMT tests, OCR shows minimal change, which is not entirely reasonable given the high preload efforts.

Permeability and consolidation coefficients obtained from CPTu continuous, CPTu dissipation, and SDMT tests demonstrate a high level of replicability, however, coefficients c and k from SPT exhibit a different behavior due their estimations are in vertical pore pressure drainage (c_v and k_v), while others are based on horizontal disposition estimations (c_h and k_h) and not all tests were conducted in the same zone.

For the study area, specific methodologies have been proposed to estimate fines content (FC), based on CPTu and SDMT measurements. To estimate FC from CPTu tests, the method proposed by Suzuki et al. is the best fit, as it yields an overall standard deviation of 2.2%. Meanwhile, to estimate the FC from SDMT tests, the method proposed by Di Buccio et al. exhibits a standard deviation close to that obtained from the CPTu tests (6%).

The Plaxis analysis indicates that the highest settlements occur during the preload construction stage (approximately 70%) compared with 90% of consolidation at 648 days. Theoretically, settlements are expected beneath the double sand layer beyond -20 masl, reaching around 90 m which is consistent with Boussinesq effort calculations which are at 90% at 80 m depth.

Acknowledgements

We extend our sincere appreciation to ESPOL for generously funding both the execution and publication of this research, as well as for lending the DMT equipment. We would also like to express our gratitude to Durán Logistics Terminal and Geocimientos S.A. for their invaluable collaboration in supplying information on the SPT and CPTu conducted during the project's construction. Their dedication and cooperation have played a pivotal role in the achievement of our research objectives.

Declaration of interest

Authors are required to disclose conflicting interests that could inappropriately bias their work. For that end, a section entitled "Declaration of interest" should be included. In case of the absence of conflicting interests, the authors should still include a declaration of interest, for which the following example could be used:

The authors have no conflicts of interest to declare. All co-authors have observed and affirmed the contents of the paper and there is no financial interest to report.

Authors' contributions

Juan Arévalo-Ochoa: Data curation, writing – original draft, formal analysis, visualization, software. Steven Muñoz-Buestán: writing, formal analysis, visualization. Davide Besenzon: Conceptualization, project administration, supervision, validation, writing – review & editing. Carlos Grau-Sacoto: data acquisition, resources. Sara Amoroso: Conceptualization, validation, writing – review & editing.

Data availability

Data generated and analyzed during the current study are not publicly available due private TLD investment, but a complete or limited dataset can be made available upon reasonable request.

List of symbols

q_t Corrected cone resistance for pore water effects

f_s Sleeve friction resistance

u_2 Water pressure at base of sleeve

u_0	Equilibrium pore water pressure
σ_v	Vertical stress
σ'_v	Effective vertical stress
σ'_p	Preconsolidation pressure
k	Permeability
k_h	Horizontal permeability
k_v	Vertical permeability
c	Consolidation coefficient
c_h	Horizontal consolidation coefficient
c_v	Vertical consolidation coefficient
p_0	First DMT corrected pressure reading
p_1	Second DMT corrected pressure reading
p_2	Third DMT corrected pressure reading
$\Delta\sigma_{ef}$	Stress increment (stress interval)
$\sigma_{1,ef}$	Stress at point 1 on the stress-strain curve
$\sigma_{2,ef}$	Stress at point 2 on the stress-strain curve
$\Delta\varepsilon$	Variation in axial deformation
ε_1	Axial deformation at point 1 on the stress-strain curve
ε_2	Axial deformation at point 2 on the stress-strain curve
w	Moisture content
γ	Unit weight
γ_w	Unit weight of water

t_{50} Time to reach 50% dissipation

t_{flex} Contraflexure time

$diss$ Dissipation

$masl$ Meters above sea level

SPT Standard penetration test

$CPTu$ Cone penetration test

$SDMT$ Seismic dilatometer test

BAP Before and after preload

AP After preload

BP Before preload

GWT Groundwater table

PI Plasticity index

PL Plastic limit

LL Liquid limit

$USCS$ Unified Soil Classification System

CH High plasticity clay

CL Low plasticity clay

C Cohesion

ϕ Friction angle

E Young modulus

I_c Soil behavior type index

Q_t Normalized cone penetration resistance

M Constrained modulus

OCR	Overconsolidation ratio
S_u	Undrained shear strength
V_s	Shear wave velocity
I_D	Material index
K_D	Horizontal stress index
E_D	Dilatometer modulus
Go	Small strain shear modulus
N_{SPT}	SPT blow count
DI	Depth interval
MTB	Mean trimmed before
MTA	Mean trimmed after
SD	Overall standard deviation
FC	Fines content
C_{FC}	Coefficient related to fines content by Boulanger & Idriss method
x_c	Coefficient related to fines content by Suzuki et al. method
x_D	Coefficient related to fines content by Di Buccio et al. method

References

Álvarez, B., Palma, H., Besenzon, D., Vera-Grunauer, X., & Amoroso, S. (2022). Geotechnical characterization of the estuarine deltaic deposits in the Guayaquil city through in situ and laboratory tests. *Soils and Rocks*, *45*(3), 1–15. https://doi.org/10.28927/SR.2022.074021

Boulanger, R. W., & Idriss, I. M. (2014). CPT and SPT based liquefaction triggering procedures. *Report No. UCD/CGM.-14*.

British Mission and Directorate General of Geology and Mines. (1979). *Geological Guayaquil 1:100000*.

Cavallaro, A. (2022). A geotechnical study for the historical heritage preservation of the City of Noto (Italy). In *Geotechnical Engineering for the Preservation of Monuments and Historic Sites III* (pp. 893–903). CRC Press. https://doi.org/10.1201/9781003308867-69

Chaiyaput, S., Ayawanna, J., Jongpradist, P., Poorahong, H., Sukkarak, R., & Jamsawang, P. (2023). Application of a cement–clay–air foam mixture as a lightweight embankment material for construction on soft clay. *Case Studies in Construction Materials*, *18*, e02188. https://doi.org/10.1016/j.cscm.2023.e02188

Di Buccio, F., Comina, C., Fontana, D., Minarelli, L., Vagnon, F., & Amoroso, S. (2023). Fines content determination through geotechnical and geophysical tests for liquefaction assessment in the Emilia alluvial plain (Ferrara, Italy). *Soil Dynamics and Earthquake Engineering*, *173*, 108057. https://doi.org/10.1016/j.soildyn.2023.108057

Fakharian, K., Bahrami, M., Kashkooli, M., Vaezian, H., & Bahrami, T. (2022). Evaluation of cyclic softening potential using CPTu and assessment with cyclic triaxial test results: A case study. In *Cone Penetration Testing 2022* (pp. 387–393). CRC Press. https://doi.org/10.1201/9781003308829-53

Fujiwara, H., & Ue, S. (1990). Effect of Preloading on Post-Construction Consolidation Settlement of Soft Clay Subjected to Repeated Loading. *Soils and Foundations*, *30*(1), 76–86. https://doi.org/10.3208/sandf1972.30.76

Kværner, J., & Snilsberg, P. (2008). The Romeriksporten railway tunnel — Drainage effects on peatlands in the lake Northern Puttjern area. *Engineering Geology*, *101*(3–4), 75–88. https://doi.org/10.1016/j.enggeo.2008.04.002

Lee, M.-J., Hong, S.-J., Choi, Y.-M., & Lee, W. (2010). Evaluation of deformation modulus of cemented sand using CPT and DMT. *Engineering Geology*, *115*(1–2), 28–35. https://doi.org/10.1016/j.enggeo.2010.06.016

Long, M., Paniagua, P., Grimstad, G., Sponås, E. B. A., Bjertness, E., & Ritter, S. (2023). Behaviour of 60-year-old trial embankments on peat. *Engineering Geology*, *323*, 107226. https://doi.org/10.1016/j.enggeo.2023.107226

Lunne, T., & Christoffersen, H. P. (1983, April 8). Interpretation of Cone Penetrometer Data for Offshore Sands. *Offshore Technology Conference*. https://doi.org/10.4043/4464-MS

Mangraviti, V., Flessati, L., & di Prisco, C. (2023). Mathematical modelling of the mechanical response of geosynthetic-reinforced and pile-supported embankments. *International Journal for Numerical and Analytical Methods in Geomechanics*, *47*(13), 2438–2466. https://doi.org/10.1002/nag.3586

Marchetti, S. (1980). In Situ Tests by Flat Dilatometer. *Journal of the Geotechnical Engineering Division*, *106*(3), 299–321. https://doi.org/10.1061/AJGEB6.0000934

Marchetti, S., Monaco, P., Totani, G., & Calabrese, M. (2001). The Flat Dilatometer Test (DMT) in Soil Investigations. *Proceedings from the Second International Flat Dilatometer Conference*.

Michaud, F., Witt, C., & Royer, J.-Y. (2009). Influence of the subduction of the Carnegie volcanic ridge on Ecuadorian geology: Reality and fiction. In *Backbone of the Americas: Shallow Subduction, Plateau Uplift, and Ridge and Terrane Collision*. Geological Society of America. https://doi.org/10.1130/2009.1204(10)

Paredes, J., & Illingworth, F. (2022). Evaluation of shear wave velocity profiles in alluvial and deltaic soils using a CPT database. In *Cone Penetration Testing 2022* (pp. 636–640). CRC Press. https://doi.org/10.1201/9781003308829-92

Paredes, J., Illingworth, F., & Luque, R. (2022). Geotechnical zoning of deltaic and alluvial soils of Guayaquil (Ecuador) using CPT and Nkt calibration based on FVT. In *Cone Penetration Testing 2022* (pp. 1042–1047). CRC Press. https://doi.org/10.1201/9781003308829-157

Ripalda, F., Falquez, D., Besenzon, D., Luque, R., Illingworth, F., & Amoroso, S. (2022). Monitoring ground improvement using in situ tests in Guayaquil, Ecuador. In *Cone Penetration Testing 2022* (pp. 1071–1076). CRC Press. https://doi.org/10.1201/9781003308829-162

Roberton, P. K. (2012). Interpretation of in-situ tests – some insights. *J.K. Mitchell Lecture*.

Robertson, P. K. (2009). CPT-DMT Correlations. *Journal of Geotechnical and Geoenvironmental Engineering*, *135*(11), 1762–1771. https://doi.org/10.1061/(ASCE)GT.1943-5606.0000119

Robertson, P. K. (2010). Estimating in-situ soil permeability from CPT & CPTu. *2nd International Symposium on Cone Penetration Testing*.

Robertson, P. K., & Cabal, K. (2022). *Guide to Cone Penetrating Testing*.

Spikings, R. A., Seward, D., Winkler, W., & Ruiz, G. M. (2000). Low-temperature thermochronology of the northern Cordillera Real, Ecuador: Tectonic insights from zircon and apatite fission track analysis. *Tectonics*, *19*(4), 649–668. https://doi.org/10.1029/2000TC900010

Suzuki, Y. (1998). Correlation between SPT and seismic CPT. *Proc. of the First International Conference on Site Characterization*.

Terzaghi, K. (1925). *Erdbaumechanik auf Bodenphysikalischer Grundlage*.

Terzaghi, K., & Peck, R. B. (1967). *Soil Mechanics in Engineering Practice: Vol. 2nd ed.*

Trenkamp, R., Kellogg, J. N., Freymueller, J. T., & Mora, H. P. (2002). Wide plate margin deformation, southern Central America and northwestern South America, CASA GPS observations. *Journal of South American Earth Sciences*, *15*(2), 157–171. https://doi.org/10.1016/S0895-9811(02)00018-4

Zhang, S., Cao, H., Xu, S., & Tao, M. (2023). Mechanical responses of subgrade with natural hard crust through an accelerated laboratory loading test on pavements model. *Case Studies in Construction Materials*, *19*, e02449. https://doi.org/10.1016/j.cscm.2023.e02449

CERTIFICACIÓN DE REVISIÓN DE PROYECTO DE TITULACIÓN

Por medio de la presente, Yo Davide Besenzon Venegas, Coordinador del Programa de Maestría en Geotecnia de la Escuela Superior Politécnica del Litoral (ESPOL), certifico que:

Con fecha 24 de febrero de 2023, los estudiantes Juan Patricio Arévalo Ochoa y Héctor Steven Muñoz Buestán con números de identificación 0706586187 y 0105356711, respectivamente, de la Cohorte 4, presentaron la propuesta de su tema de titulación al Comité Académico del programa. Posteriormente, con fecha 20 de noviembre de 2023, el Comité revisó y aprobó la propuesta mediante la resolución FICT-CA-GEOTEC-037-2023, cumpliendo con los requisitos establecidos para la aprobación del tema.

A partir de dicha aprobación, los estudiantes mantuvieron reuniones periódicas con el tutor designado, Davide Besenzon Venegas, para la elaboración y desarrollo de su proyecto de titulación, siguiendo los lineamientos establecidos por el programa. Con fecha 25 de noviembre de 2023, los estudiantes presentaron y sustentaron su proyecto de titulación ante el tribunal evaluador asignado, cumpliendo con el proceso formal de evaluación académica.

Por lo tanto, en calidad de Coordinador del Programa de Maestría en Geotecnia, certifico que el trabajo de titulación denominado **"Análisis comparativo de ensayos in-situ previo y post colocación de precargas en el Terminal Logístico Durán"**, realizado por los estudiantes Juan Patricio Arévalo Ochoa y Héctor Steven Muñoz Buestán con números de identificación 0706586187 y 0105356711, respectivamente, ha sido revisado y evaluado conforme a los lineamientos y estándares establecidos por el programa.

Debido a circunstancias externas, no ha sido posible obtener las firmas de los involucrados (estudiante, tutor(es) y/o evaluadores). No obstante, en calidad de Coordinador del Programa, certifico que el proyecto cumple con los requisitos académicos y ha sido revisado para su presentación y archivo institucional.

Atentamente,

Firmado electrónicamente por:
ANDRES EDUARDO
GUZMAN VELASQUEZ

M. Sc. Andrés Eduardo Guzmán Velásquez
Coordinador General de Postgrados FICT